HYDROLOGICAL PROCESSES
Hydrol. Process. **23**, 2004–2011 (2009)
Published online 22 May 2009 in Wiley InterScience
(www.interscience.wiley.com) DOI: 10.1002/hyp.7343

Hydrologic drainage of the Greenland Ice Sheet

Sarah M. Lewis[1]*,† and Laurence C. Smith[1,2]

[1] *Department of Geography, University of California, Los Angeles, CA, USA*
[2] *Department of Earth & Space Sciences, University of California, Los Angeles, CA, USA*

Abstract:

A simple hydrologic drainage network for the Greenland Ice Sheet is modelled from available digital elevation models (DEMs) of bedrock, and surface topography and assumptions of hydrostatic water pressure, uniform hydraulic conductivity, and no conduit flow within the ice sheet. As such, it is a first-order model best suited for broad-scale hydrological assessment. Results identify 293 distinct hydrologic basins (185–117 000 km^2) together with their 'realized' (wet) and 'unrealized' (dry) drainage patterns. Intersection with 1991–2000 Polar MM5 (PMM5) mesoscale climate model hindcasts of meltwater runoff suggest that these basins route varying amounts of water to the ice edge, ranging from 0 to 16 km^3 annually and totalling 242 km^3/year for the entire ice sheet. Regionally speaking, average annual volumetric meltwater production (km^3/year) is highest in southwest and lowest in northeast Greenland, with greater hydrologic activity in western regions than in eastern regions for a given latitude. The extent to which meltwater truly reaches the ice margin as modelled is difficult to test. However, the simulated flow outlet locations show qualitative agreement with the locations of 460 observed meltwater outlets (proglacial lakes, streams, and rivers; and sediment plumes into fjörds) mapped continuously along the ice sheet perimeter. On average, about 36% of the modelled drainage network was activated (i.e. received water) over the 1991–2000 study period. Remaining areas, barring dynamic changes to ice-surface topography, would presumably activate if surface melt penetrates deeper into the ice sheet interior. Both new datasets are freely available for scientific use at the National Snow and Ice Data Center (ftp://sidads.colorado.edu/pub/DATASETS/parca/nsidc-0372-hydrologic-outlets; ftp://sidads.colorado.edu/pub/DATASETS/parca/nsidc-0371-hydrologic-sub-basins). Copyright © 2009 John Wiley & Sons, Ltd.

KEY WORDS Greenland Ice Sheet; hydrology; drainage network; GIS; meltwater; hydrostatic

Received 8 September 2008; Accepted 24 March 2009

INTRODUCTION

Recent studies suggest that the Greenland Ice Sheet is thinning at an alarming rate (Krabill *et al*., 2004, Luthcke *et al*., 2006; Rignot *et al*., 2006; Bamber *et al*., 2007) and may contribute up to 54 cm to global sea-level rise by 2100 (Pfeffer *et al*., 2008). While most of these mass losses are dynamic, surface melting may also affect glacier dynamics by directing meltwater to the glacier bed to affect resistance to glacier sliding, and basal melting could influence the buttressing effect of floating glacial tongues (Thomas *et al*., 2003; Box *et al*., 2007; McMillan *et al*., 2007; Das *et al*., 2008). Using passive microwave satellite data from 1979 to 1999, an analysis of the extent of ice sheet melt revealed a positive melt trend of 1% per year (Abdalati and Steffen, 2001), and more recent studies document the record melt years of 2002, 2005 and 2007 (Mote, 2007; Steffen *et al*., 2007; Hanna *et al*., 2008). New studies have raised the possibility that increased surface melting could accelerate ice-flow velocities, thereby increasing ice sheet contributions to sea level-rise owing to a greater prevalence of meltwater at the bed (Zwally *et al*., 2002; Alley *et al*., 2005; Fountain *et al*., 2005; Harper *et al*., 2007; Bartholomaus *et al*., 2008). Furthermore, between 1996 and 2000 widespread glacier acceleration occurred below 66° North and by 2005 the northern line of observed glacier acceleration had expanded to 70° North (Rignot *et al*., 2006), contemporaneous with increased surface melting (Hall *et al*., 2008). Joughin *et al*. (2008) and Shepherd *et al*. (2009) have now identified a direct link between seasonal surface melting and ice sheet sliding velocity. In light of such observations, hydrological studies of Greenland are increasingly directed towards the mechanisms by which meltwater penetrates and exits the ice sheet. However, scientific understanding of englacial and subglacial water flow paths within the ice sheet remains poor.

Basic hydraulics dictate that ice sheet surface and bedrock topography strongly influence the pattern of hydrologic flow drainage networks that develop annually on top of or within the ice sheet (Paterson, 1994). Here we use the hydraulic potentiometric surface, derived from Greenland's surface and bedrock topography, to create a simple flow-path model in a geographic information system (GIS). Previous studies have used a GIS approach to delineate major drainage basins from ice sheet surface topography and balance flux (Hardy *et al*., 2000), but ours is the first to incorporate bedrock topography in

* Correspondence to: Sarah M. Lewis, Department of Environmental Science, Policy, and Management, University of California, Berkeley, 137 Mulford Hall #3114, Berkeley, CA 94720-3114, USA.
E-mail: sarahlewis@berkeley.edu
† Now at Department of Environmental Science, Policy, and Management, University of California, Berkeley, CA, USA.

the creation of a modelled flow network. As such, the resulting drainage network traces the top of the hydraulic potentiometric surface, which underlies the physical ice surface just as a groundwater table does beneath *terra firma* terrain. Flow 'divides' delineate distinct hydrologic sub-basins; and coalesced flow paths indicate modelled 'flow outlets' where they intersect the perimeter of the ice sheet.

Following derivation of the drainage pattern, two other hydrologic datasets are used to drive and evaluate the modelled flow network, namely (1) a map of long-term average annual meltwater runoff production across the ice sheet surface (Box *et al*., 2004) and (2) a new point-based dataset, created specifically for this study, of 460 observed meltwater outlets, including streams and other physical evidence of meltwater release, mapped continuously around the entire periphery of the ice sheet using high-resolution satellite imagery. The latter dataset is particularly novel because the spatial distribution of such features has not previously been examined for the Greenland Ice Sheet.

METHODS

Two quite different methodologies were used in this analysis. The first was to identify 'potential' hydrologic flow networks and sub-basins across Greenland using its hydraulic potentiometric surface and then intersect them with Polar MM5 (PMM5) climate model simulations of meltwater production at the ice sheet surface. Therefore, the resultant 'watersheds' and 'flow networks' are (1) activated only where meltwater is actually produced; (2) reflect englacial as well as supra-glacial flow; and (3) predict where liquid water is likely to flow through and exit from the ice sheet. The second methodology was to use satellite data to map the spatial distribution of observed meltwater outlets along the ice sheet margin, for comparison with the modelled meltwater flow outlet locations.

Generation of hydrologic flow networks and sub-basins

Digital elevation models (DEMs) of ice surface and bedrock topography (Bamber *et al*., 2001) were used to estimate the hydraulic potentiometric surface for Greenland, which accounts for the effects of ice overburden pressure (i.e. hydrostatic pressure), surface topography, and underlying bedrock topography (Paterson, 1994):

$$\varphi \simeq \rho_{\mathrm{i}}\, g(h_{\mathrm{s}} + 0{\cdot}1\ y) \tag{1}$$

where φ is the modelled elevation of the potentiometric surface; ρ_{i} is the density of ice; g is the gravitational constant; h is the ice sheet surface elevation; and y is the bedrock elevation (Paterson, 1994) (Figure 1). This model assumes that the basal water pressure is balanced by the ice overburden pressure ($P_{\mathrm{w}} \approx P_{\mathrm{i}}$). The pressure field is thus hydrostatic and does not consider conduit or fracture flow (e.g. in moulins) nor does it incorporate any type of fluid flow dynamics. Note that the surface slope dominates direction of water flow unless bedrock slope is substantially greater than the surface slope. The generated potentiometric hydraulic surface has a resolution of 5 km and reflects variations in both surface and bedrock topography (Figure 1).

Next, the potentiometric surface was used to model the most likely flow drainage network for the entire ice sheet in a GIS (ARC/INFO v.9·2) as follows: First, a cell-based continuous grid of 'flow direction' was defined by assigning each cell one of eight directions

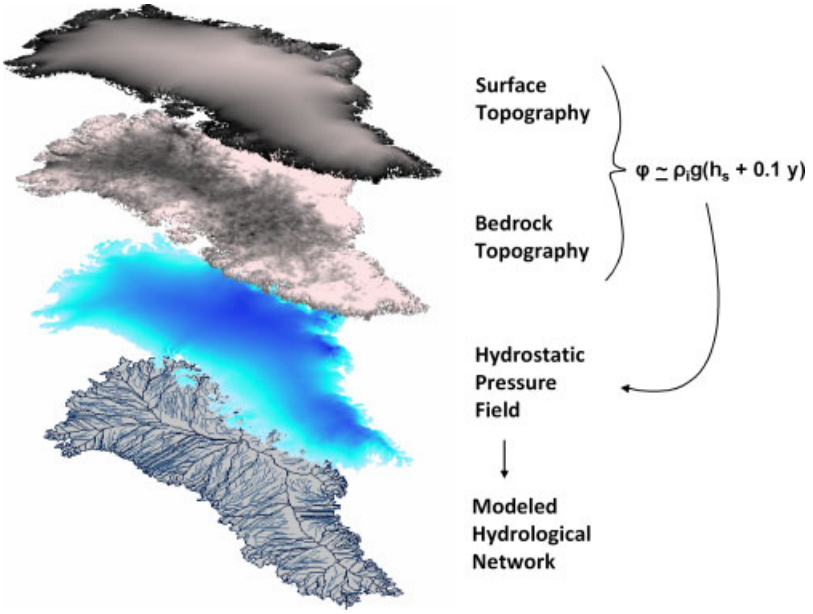

Figure 1. Creation of hydrological model. Digital elevation models (DEMs) of ice-surface and bedrock topography (Bamber *et al*., 2001) were used to estimate the hydrostatic pressure field of Greenland (φ), which accounts for the effects of ice overburden pressure (i.e. hydrostatic pressure) (ρ_{i}), surface topography (h), and underlying bedrock topography (y) (Paterson, 1994). Using the 5-km potentiometric grid, a modelled flow network for Greenland's ice sheet was created with the hydrological tools in GIS (ARC/INFO 9·2)

DOI: 10.1002/hyp

to its steepest down slope neighbour. Next, a 'flow accumulation' grid was created to identify how many upslope cells flowed into any given cell, thereby creating a surface of possible upslope flow area draining into each cell. Finally, a watershed delineation was applied to the previous grids, allowing identification of both flow divides and hydrologic sub-basins. Owing to the relatively coarse input DEMs (5 km) and the broad-scale objectives of this analysis, sub-basins less than 100 km^2 in area were removed from the dataset. Along each sub-basin's intersection with the ice sheet perimeter, the location of maximum flow accumulation—i.e. the 'flow outlet' for that particular basin—was identified. A 50-km buffer was defined around each modelled meltwater outlet enabling later counting of observed meltwater outlets (see next section) within the vicinity of each modelled outlet.

The above procedure identifies numerous hydrologic sub-basins within the ice sheet, each with its own drainage network converging to a single outlet exiting the ice sheet. However, it does not discern between 'realized' flow paths, which require melting to occur, and 'unrealized' flow paths, which do not. To identify those areas of the modelled drainage network most likely to be potentially active, the network was intersected with a map of long-term (10 year average, 1991–2000, 24 km resolution) average annual surface meltwater runoff production based on Polar MM5 mesoscale model simulations and *in situ* Automated Weather Station data (Box *et al*., 2004). The meltwater runoff data were resampled to the 5-km potentiometric hydraulic surface grid spacing, summed for each hydrologic sub-basin, and normalized by the sub-basin's total area to yield specific runoff (cm/year) and also by the area of the basin experiencing melt to yield melt intensity (cm/year) for each of the 293 sub-basins. Owing to the large size of the sub-basins, the native 24-km resolution of the PMM5 data was sufficient. Note that we do not consider basal melting which generates a small but consistent amount of meltwater that may well be active within our 'unrealized' modelled flow paths. The GIS database containing all of the modelled hydrologic sub-basin and flow drainage patterns is now freely available for scientific use at the National Snow and Ice Data Center [Lewis and Smith, 2009; Dataset freely available for scientific use at the National Snow and Ice Data Center (ftp://sidads.colorado.edu/pub/DATASETS/parca/nsidc-0371-hydrologic-sub-basins)].

Mapping of meltwater features around the ice sheet perimeter

Observed meltwater outlets along the edge of the Greenland Ice Sheet were manually digitized via photointerpretation of Landsat Enhanced Thematic Mapper Plus (ETM+) panchromatic satellite imagery with a pixel resolution of 15 m (http://www.landcover.org) and high-resolution satellite imagery available from GoogleEarth. Mapped outlets included (1) proglacial streams and rivers emerging from the ice sheet (length scale >1 km); (2) proglacial lakes touching the ice edge at glacier tongues or clearly connected to it via streams or rivers (length scale >3 km), and (3) sediment-rich plumes exiting tidewater glaciers into fjörds (Figure 3). These observed hydrologic outlet features represent direct evidence of ice sheet drainage and are hereafter referred to as 'confirmed meltwater outlets.' A total of 460 confirmed meltwater outlets were mapped in the GIS as point locations and summed within each 50-km radius of the 293 modelled meltwater outlets outlined in the previous section.

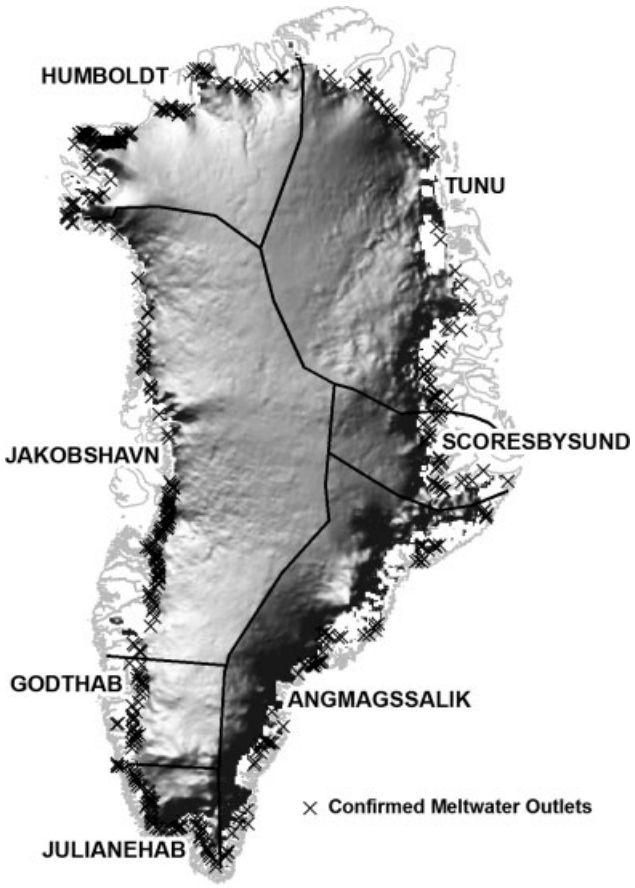

Figure 2. Confirmed meltwater outlet locations overlaid on shaded relief of the 5-km resolution potentiometric surface of the Greenland Ice Sheet

Tidewater glaciers (and other direct ice-ocean contacts) lacking sediment plumes are potential but unproven sources of meltwater release from the ice sheet. A further 431 such locations were mapped as 'possible meltwater outlets' but excluded from further analysis. Because exact satellite acquisition dates were not available in the image datasets used, it is unknown to what extent early season imaging may have caused some features to be called 'possible' meltwater outlets that would otherwise have been 'confirmed' if viewed later in the year. However, based on illumination and relatively snow-free conditions seen in nearly all images, most images were likely acquired between mid and late summer. No satellite data were available for a small area of the northern Tunu region (approximately 1% of the study area); thus this area was excluded from study. A GIS database

DOI: 10.1002/hyp

Table I. Regional comparison of confirmed meltwater outlet presence and density, specific meltwater production (average annual meltwater depth per total sub-basin area; cm/year), and meltwater intensity (average annual meltwater depth per average thawed surface area; cm/year)

Region	Region area (km^2)	Melt area (km^2)	% Melt area (%)	# Confirmed meltwater outlets identified	# Potential meltwater outlets identified	# Hydrologic drainage basins	Average annual meltwater production (volumetric, km^3/year)	Average annual specific runoff within entire basin area (cm/year)	Average annual melt intensity within thawed basin area (cm/year)	Average # confirmed meltwater outlets within 50 km radius from modelled drainage basin outlet
Angmagssalik	324 822	56 438	17	69	251	96	42·4	13	75	4·00
Godthab	114 719	38 021	33	33	3	14	35·1	31	92	7·57
Humboldt	289 629	127 424	44	116	46	42	16·6	6	13	8·21
Jakobshavn	711 844	196 031	28	101	62	54	85·4	12	44	5·94
Julianehab	68 324	32 030	47	58	25	22	37·5	55	117	11·59
Scorebysund	132 743	29 225	22	32	24	26	8·3	6	28	4·42
Tunu	634 235	137 036	22	51	20	39	16·8	3	12	2·69
Eastern Humboldt	223 333	92 205	41	38	12	15	7·9	4	9	5·20
Western Humboldt	66 297	34 902	53	78	34	27	8·6	13	25	9·89

Specific runoff = average annual meltwater depth per total sub-basin area.
Melt intensity = average annual meltwater depth per average thawed surface area.
All units are in liquid water equivalent.

containing locations of all of the remotely sensed confirmed and potential meltwater outlets is freely available for scientific use at the National Snow and Ice Data Center [Lewis and Smith, 2009; dataset freely available for scientific use at the National Snow and Ice Data Center (ftp://sidads.colorado.edu/pub/DATASETS/parca/nsidc-0372-hydrologic-outlets)].

RESULTS

In total 293 hydrologic basins, each with a distinct drainage network delivering flow to a modelled meltwater outlet at the edge of the ice sheet, were identified from this analysis (Figure 4, Table I). Realized ('wet', solid lines on Figure 4) and unrealized ('dry', dashed lines on Figure 4) drainage patterns were also delineated based on the average ice sheet melt extent during the 1991–2000 study period. Results are herein discussed in accordance with Greenland's seven climatic regions (Angmagssalik, Godthab, Humboldt, Jakobshavn, Julianehab, Scoresbysund, and Tunu) as designated by Ohmura and Reeh (1991) (Figure 2).

The Angmagssalik region, owing to its relatively complex terrain and steep potentiometric surface, contains the greatest number of basins (93) despite being second largest in size (324 822 km^2, after the Jakobshavn region which covers 711 844 km^2 and contains 54 basins) (Figure 2). However, Jakobshavn basins generate the most total meltwater, producing ~85 km^3 annually versus ~42 km^3 in Angmagssalik (**Table I**). Tiny Julianehab (68 324 km^2 with only 22 basins) generates nearly as much meltwater as Angmagssalik (~38 km^3) despite having only one-fifth its surface area, owing to its extremely high average melt intensity (total annual meltwater volume per unit thawed area, 117 cm/year) and melt area (47%). Similarly, specific meltwater runoff (total meltwater volume per entire sub-basin area, cm/year) and melt intensity are highest in Julianehab (55 and 117 cm/year, respectively) and Godthab (31 and 92 cm/year, respectively) and lowest in Humboldt (6, 13 cm/year) and Tunu (3, 12 cm/year) regions. In the east, Scoresbysund, as compared to its neighbouring regions Tunu and Angmagssalik, exhibits median specific meltwater runoff and melt intensity (6, 28 cm/year), thereby illustrating the latitudinal gradient between the two regions.

Manual photointerpretation of all available satellite data identifies 460 confirmed meltwater outlets, 350 of which visibly drain to the ocean (Figures 2, 3, Tables I and II). An additional 431 possible meltwater outlets were also identified. Of these, a majority (252) occur in the Angmagssalik region, an area of abundant tidewater glaciers and floating ice. Julianehab has the highest density of confirmed meltwater outlets in the vicinity of the modelled outlets of this study (an average of 11·59 outlets per 50 km radius of a modelled outlet) (last column, Table I). In contrast, Tunu has the lowest with an average of 2·69 confirmed meltwater outlets near

DOI: 10.1002/hyp

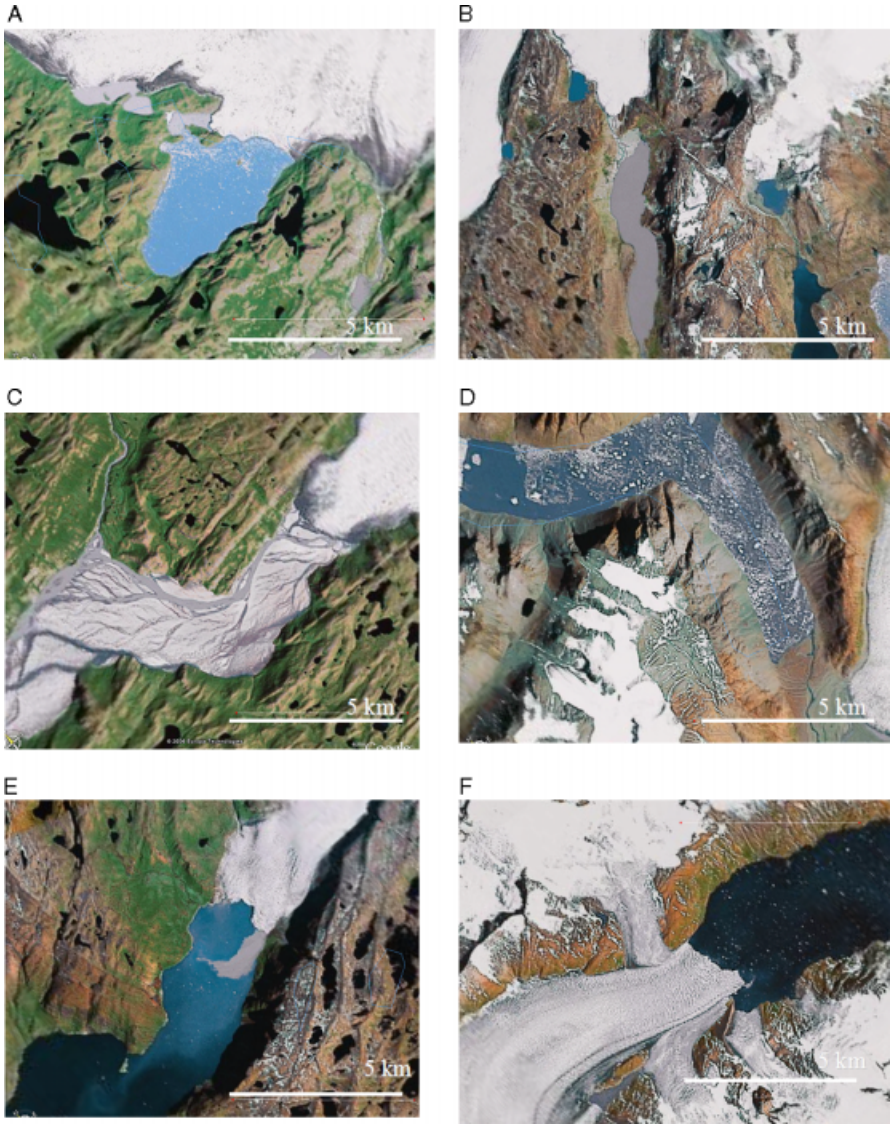

Figure 3. Examples of observed meltwater outlets. (A) Turbid proglacial lake, (B) river to proglacial lake, (C) river, D) proglacial lake to river, E) sediment into Fjörd, F) unconfirmed 'Possible' outlet

Table II. Regional distribution of confirmed meltwater outlets mapped using high-resolution satellite imagery

Confirmed meltwater outlet	Angmagssalik	Godthab	Humboldt	Jakobshavn	Julianehab	Scoresbysund	Tunu	Western Humboldt	Eastern Humboldt	All
Sediment into Fjörd	11	1	1	10	2	1	0	1	0	26
Turbid Proglacial Lake	24	15	3	36	11	3	7	3	0	99
River	24	14	103	34	29	25	35	71	32	264
Proglacial Lake into River	8	3	4	21	15	2	7	3	1	60
River into Proglacial Lake	2	0	5	0	1	1	2	0	5	11
All	69	33	116	101	58	32	51	78	38	460

modelled outlets. These differences largely correlate to the respective wet and dry climates of these regions as well as meltwater drainage patterns. However, further differences in the distribution of meltwater outlets are introduced by available land area, prevalence of tidewater glaciers, and geomorphology. For example, of the 116

DOI: 10.1002/hyp

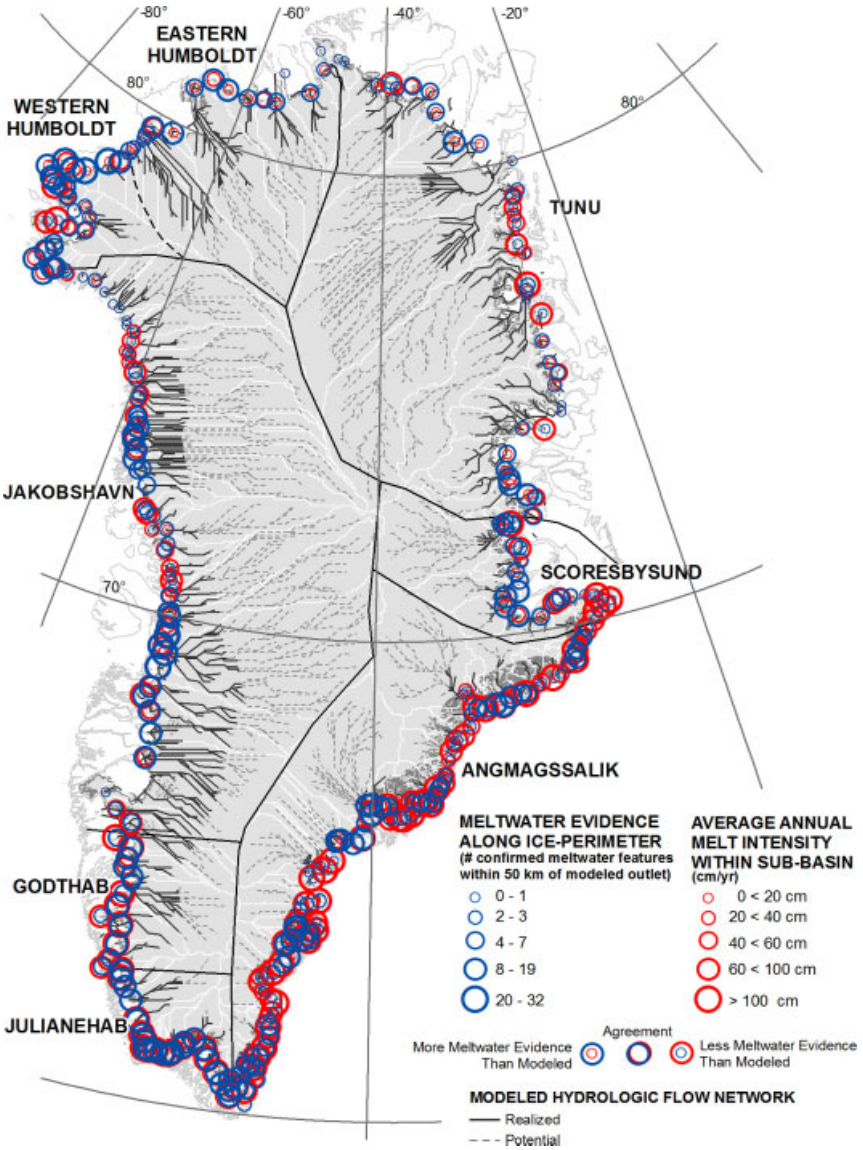

Figure 4. Meltwater evidence along the ice sheet perimeter (number of confirmed meltwater features within a 50-km vicinity of a modelled outlet) versus meltwater intensity (total annual meltwater volume per unit thawed area, cm) within each hydrologic sub-basin, illustrating that rivers, streams, and proglacial lakes are generally more prevalent near 'wet', hig–producing modelled meltwater outlets than 'dry', low-producing outlets (as seen in similar size variations in blue and red circles). Modelled hydrologic flow network delineates realized ('wet', solid lines) and unrealized ('dry', dashed lines) drainage patterns

confirmed meltwater outlets in the Humboldt region, 103 are rivers exiting the ice sheet, owing likely to the wide coastline and few tidewater glaciers in this area.

Despite the markedly different properties of the two datasets, a general, if qualitative, agreement exists between modelled meltwater outlets and confirmed meltwater outlets. In general, rivers, streams, and proglacial lakes are more prevalent near 'wet', high-producing modelled meltwater outlets and less prevalent near 'dry', low-producing modelled meltwater outlets (see similar size variations in blue and red circles in Figure 4 and Figure 5). The Julianehab and Godthab regions display the highest runoff conditions in both modelled and confirmed meltwater outlets, whereas the Tunu and Scoresbysund regions have the least (Figure 4, Figure 5). However, divergence between the two datasets occurs in the Angmagssalik region, where meltwater outlets are difficult to detect owing to a high abundance of tidewater glaciers, low available land area, and abundant floating ice (causing large red circles and small blue circles in Figure 4 and divergence in Figure 5), and also the Humboldt region (see large red circles, small blue circles, Figure 4). Interestingly, this apparent Humboldt divergence is reduced if the region is split into an eastern and western part (Table II; last two columns, Figure 5).

DISCUSSION AND CONCLUSION

The results of this simple, broad-scale hydrologic model are in relative harmony with the regional climatic zones of Ohmura and Reeh (1991), which state that the southwest of Greenland is significantly wet and the northeast significantly dry (Ohmura and Reeh, 1991). Regionally

DOI: 10.1002/hyp

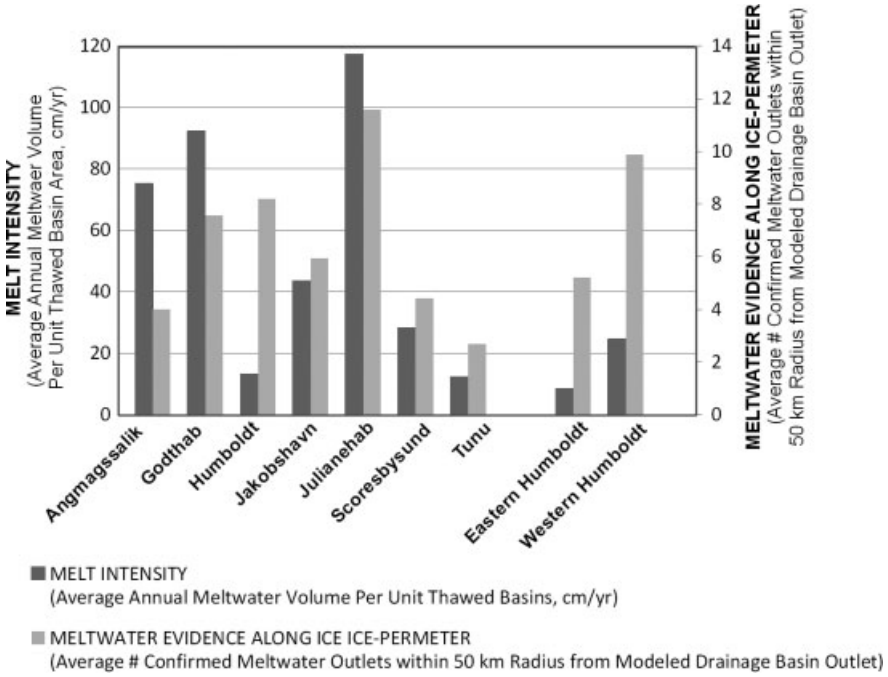

Figure 5. Regional averages of meltwater intensity (average annual meltwater volume per unit thawed basin, cm/year) versus meltwater evidence (average number of confirmed meltwater outlets within 50 km radius from modelled drainage basin outlet)

speaking, average annual volumetric meltwater production (km^3/year) is highest in southwest and lowest in northeast Greenland, with greater hydrologic activity in western regions than in eastern regions for a given latitude (Table I). Melt intensity (average annual meltwater volume per unit thawed area) is highest in the southwest and lowest in the northeast. Specific runoff (average annual meltwater volume per entire sub-basin area) was correspondingly high in Julianehab (55 cm/year) and low in Tunu (3 cm/year). Over a 10-year period, Tunu averaged the lowest melt intensity (12 cm/year) and Julianehab averaged the highest (117 cm/year).

It is difficult to test the validity of any hydrologic model for Greenland in the absence of field data on stream discharge, lake stage, or other hydrologic observations of flows exiting the ice sheet. However, except for the Angmagssalik and Humboldt regions, a general agreement between modelled meltwater outlets and confirmed meltwater outlets lends qualitative support to this model. The main exception to this is in Angmagssalik where high melt production suggests abundant runoff, but the physical evidence of this is sparse owing to limited available land area (precluding development of lakes and streams) and high density of floating ice (obscuring imaging of sediment plumes from space). Although Angmagssalik contains more unconfirmed 'potential' meltwater outlets than any other part of Greenland (251, Table I), we speculate that significant, if unobserved water may exit the ice sheet through these pathways.

Neither floating ice nor a lack of land area is problematic in the Humboldt region, where divergence between observed and modelled hydrology is also found (Figure 4, Figure 5). Humboldt exhibits a relatively high number of confirmed outlets relative to its short coastline and low runoff production, particularly in its western half (78 confirmed meltwater outlets, third only to the southern and warmer Julianehab and Angmagssalik regions). In contrast, its eastern half has only 38 confirmed outlets. This east–west contrast is also reflected in a distinct bifurcation of melt intensity with low but more intense values in the west (13 cm/year) and significantly less intense melting in the east (4 cm/year), a pattern that is likely explained by low elevations in the latter. Therefore, from a hydrological standpoint the region should be split in half, into an Eastern and Western Humboldt region. Thus partitioned, Eastern Humboldt, like Tunu, would be considered a dry zone; and the observed dichotomy between Greenland's more water-productive west coast and less water-productive east coast would be reflected in the western and eastern halves, respectively.

Relative to the rest of the ice sheet, Tunu (and the proposed Eastern Humboldt) represents the most hydrologically inactive area of Greenland (22% melt area and 3 cm/year specific runoff, vs 47% and 55 cm/year for Julianehab, Table I). Owing to its large size, this area technically poses the greatest 'untapped potential' for increased runoff delivery to the global ocean. However, it is also one of the most perpetually frozen areas of Greenland. It is important to note that the vast majority of the ice sheet remains hydrologically inactive: on average, only ~36% of its surface experienced melting over the 1991–2000 study period; and only 53% melted in 2007, the most extreme year on record (Mote, 2007; Steffen *et al*., 2007; Hanna *et al*., 2008).

While approximately two-thirds of Greenland do not experience sustained melt, the dashed drainage patterns on Figure 4 represent 'potential' hydrologic flow paths that are currently unrealized except for basal melting.

DOI: 10.1002/hyp

Barring changes in surface topography due to thinning or other ice dynamics, they are the broad-scale drainage patterns that would likely activate, should surface melting increase in the future.

ACKNOWLEDGEMENTS

Funding was provided by the NASA Cryosphere Sciences Program grant NNG05GN89G, managed by Seelye Martin. The idea for this study arose from stimulating discussions with Kurt Cuffey at the University of California, Berkeley, Department of Geography. Jason Box at The Ohio State University kindly provided PMM5 melt simulations.

REFERENCES

Abdalati W, Steffen K. 2001. Greenland ice sheet melt extent: 1979–1999. *Journal of Geophysical Research* **106**(D24): 33–983–33–988.

Alley RB, Dupont TK, Parizek BR, Anandakrishnan S. 2005. Access of surface meltwater to beds of sub-freezing glaciers: preliminary insights. *Annals of Glaciology* **40**: 8–14.

Bamber JL, Alley RB, Joughin I. 2007. Rapid response of modern day ice sheets to external forcing. *Earth and Planetary Science Letters* **257**: 1–13.

Bamber JL, Layberry RL, Gogenini SP. 2001. A new ice thickness and bed data set for the Greenland ice sheet 1: measurement, data reduction, and errors. *Journal of Geophysical Research* **106**(D24): 33–773–33–780.

Bamber JL, Layberry RL, Gogenini SP. 2001. A new ice thickness and bed data set for the Greenland ice sheet 2: Relationship between dynamics and basal topography. *Journal of Geophysical Research* **106**(D24): 33781–33788.

Bartholomaus TC, Anderson RS, Anderson SP. 2008. Response of glacier basal motion to transient water storage. *Nature Geoscience* **1**(1): 33–37.

Box JE, Bromwich DH, Bai LS. 2004. Greenland ice sheet surface mass balance for 1991–2000: Application of Polar MM5 mesoscale model and in-situ data. *Journal of Geophysical Research* **109**(D16105): 1–21.

Box JE, Ski K. 2007. Remote sounding of Greenland supraglacial melt lakes: implications for subglacial hydraulics. *Journal of Glaciology* **53**(181): 257–265.

Das SB, Joughin I, Behn M, Howat IM, King MA, Lizarralde D, Bhatia MP. 2008. Fracture propagation to the base of the Greenland ice sheet during supraglacial lake drainage. *Sceince* **230**: 778–781.

Fountain AG, Jacobel RW, Schlichting R, Jansson P. 2005. Fractures as the main pathways of water flow in temperate glaciers. *Nature* **433**: 618–620.

GoogleEarth®. 2005. http://earth.google.com/.

Hall DK, Williams RS, Jr, Luthcke SB, DiGirolamo NE. 2008. Greenland Ice Sheet surface temperature, melt and mass loss: 2000–2006. *Journal of Glaciology* **54**(184): 81–93.

Hanna E, Irvine-Fynn T, Wise S, Huybrechts P, Steffen K, Huff R, Cappelen J, Shuman C, Griffiths M. 2008. Increased runoff from melt from the Greenland ice sheet: a response to global warming. *Journal of Climate* **21**: 331–341.

Hardy RJ, Bamber JL, Orford S. 2000. The delineation of drainage basins on the Greenland ice sheet for mass-balance analyses using a combined modeling and geographical information system approach. *Hydrological Processes* **14**: 1931–1941.

Harper JT, Humphrey NF, Pfeffer WT, Lazar B. 2007. Two modes of accelerated glacier sliding related to water. *Journal of Geophysical Research Letters* **34**(L12503): 1–5.

Joughin I, Das SB, King MA, Smith BE, Howat IM, Moon T. 2008. Seasonal speedup along the western flank of the Greenland Ice Sheet. *Science* **320**(5877): 781–783.

Krabill W, Hanna E, Huybrechts P, Abdalati W, Cappelen J, Csatho B, Frederick E, Manizade S, Martin C, Sonntag J, Swift R, Thomas R, Yungel J. 2004. Greenland Ice Sheet: increased coastal thinning. *Journal of Geophysical Research Letters* **31**(L24402): 1–4.

Lewis S, Smith L. 2009. *Hydrologic Outlets of the Greenland Ice Sheet*. National Snow and Ice Data Center. Digital media: Boulder, CO, USA.

Lewis S, Smith L. 2009. *Hydrologic Sub-basins of Greenland*. National Snow and Ice Data Center. Digital media: Boulder, CO, USA.

Luthcke SB, Zwally HJ, Abdalati W, Rowlands DD, Ray RD, Nerem RS, Lemoine FG, McCarthy JJ, Chinn DS. 2006. Recent Greenland ice mass loss by drainage system from satellite gravity observations. *Science* **314**(5803): 1286–1289.

McMillan M, Nienow P, Shepard A, Benham T, Sole A. 2007. Seasonal evolution of supra-glacial lakes on the Greenland Ice Sheet. *Earth and Planetary Science Letters* **262**: 484–492.

Mote T. 2007. Greenland surface melt trends 1973–2007: evidence of a large increase in 2007. *Geophysical Research Letters* **34**: 1–5.

NASA Landsat Program. U.S. Geological Survey. Landsat ETM+, Scene, WRS-2. Global Land Cover Facility (GLCF), USGS: Sioux Falls, South Dakota. <http://www.landcover.org>.

Ohmura A, Reeh N. 1991. New precipitation and accumulation maps for Greenland. *Journal of Glaciology* **37**(125): 140–148.

Paterson WSB. 1994. *The Physics of Glaciers* (3rd edn). Pergamon Press: Oxford.

Rignot E, Kanagaratnam P. 2006. Changes in the Velocity Structure of the Greenland Ice Sheet. *Science* **311**: 986–990.

Pfeffer WT, Harper JT, O'Neel S. 2008. Kinematic constraints on glacier contributions of 21st-century sea-level rise. *Science* **321**(5894): 1340–1343.

Shepherd A, Hubbard A, Nienow P, King M, McMillan M, Joughin I. 2009. Greenland ice sheet motion coupled with daily melting in late summer. *Geophysical Research Letters* **36**(L01501): DOI:10.1029/2008GL035758.

Steffen K, Huff R, Behar A. 2007. Arctic warming, Greenland melt and moulins. *Eos Transactions American Geophysical Union* **88**(52): Fall Meet. Suppl., Abstract G33B-1242.

Thomas RH, Abdalati W, Frederick E, Krabill WB, Manizade S, Steffen K. 2003. Investigation of surface melting and dynamic thinning on Jakobshavn Isbrae, Greenland. *Journal of Glaciology* **49**(165): 231–239.

Zwally H, Abdalati W, Herring T, Larson K, Saba J, Steffen K. 2002. Surface melt–induced acceleration of Greenland ice sheet flow. *Science* **297**: 218–222.